

High temperature thermal conductivity of platinum microwire by 3ω method

Cite as: Rev. Sci. Instrum. **81**, 114904 (2010); <https://doi.org/10.1063/1.3496048>

Submitted: 23 August 2010 • Accepted: 09 September 2010 • Published Online: 09 November 2010

Rudra P. Bhatta, Sezhian Annamalai, Robert K. Mohr, et al.



[View Online](#)



[Export Citation](#)

ARTICLES YOU MAY BE INTERESTED IN

[Thermal conductivity measurement from 30 to 750 K: the \$3\omega\$ method](#)

Review of Scientific Instruments **61**, 802 (1990); <https://doi.org/10.1063/1.1141498>

[\$3\omega\$ method for specific heat and thermal conductivity measurements](#)

Review of Scientific Instruments **72**, 2996 (2001); <https://doi.org/10.1063/1.1378340>

[\$1\omega\$, \$2\omega\$, and \$3\omega\$ methods for measurements of thermal properties](#)

Review of Scientific Instruments **76**, 124902 (2005); <https://doi.org/10.1063/1.2130718>

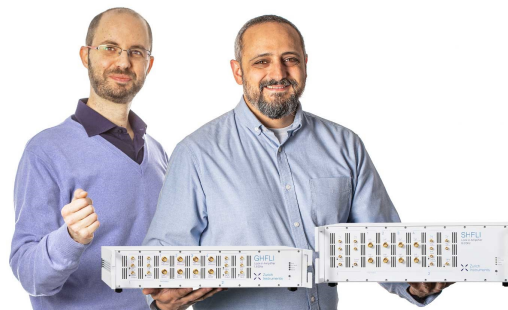
Webinar

Meet the Lock-in Amplifiers
that measure microwaves

Oct. 6th – Register now



Zurich
Instruments



High temperature thermal conductivity of platinum microwire by 3ω method

Rudra P. Bhatta,¹ Sezhian Annamalai,¹ Robert K. Mohr,¹ Marek Brandys,¹ Ian L. Pegg,^{1,2} and Biprodas Dutta^{1,2}

¹Vitreous State Laboratory, The Catholic University of America, Washington, DC 20064, USA

²ZT3 Technologies, Inc., Thousand Oaks, California 91362, USA

(Received 23 August 2010; accepted 9 September 2010; published online 9 November 2010)

The 3ω method for thermal conductivity measurement has emerged as an effective technique applicable to micro/nanowires and thin films. This paper describes the adaptation of the method to temperatures as high as 725 K enabling reliable thermal conductivity measurements on such samples for which previously published methods have been found inadequate. In the technique, a sample wire is heated by applying a sinusoidal current at an angular frequency ω , which causes a temperature and resistance variation at an angular frequency, 2ω , leading to a voltage signal at 3ω . The sample is connected as a four-terminal resistor to a digital lock-in amplifier, which is used to detect the in-phase and out-of-phase 3ω voltages resulting from the applied 1ω current. The data are fitted by varying the values of the thermal resistance and diffusion time, both of which are functions of thermal conductivity. Measurements are made at steady state temperatures between 300 and 725 K. Meaningful measurements at elevated temperatures require that thermal losses be understood and minimized. Conduction losses are prevented by suspending the sample above the mounting substrate. Convection losses are minimized by maintaining a vacuum of $\sim 10^{-5}$ torr inside the sample chamber. To minimize radiation losses, an appropriately sized sample is shrouded with a double heat-shield, with the inner shield temperature near that of the sample. Using the 3ω method, the thermal conductivity of platinum was determined to vary between 71.8 and 80.7 $\text{Wm}^{-1} \text{K}^{-1}$ over the temperature range of 300 to 725 K, in agreement with published values measured for bulk samples. © 2010 American Institute of Physics. [doi:10.1063/1.3496048]

I. INTRODUCTION

The study of the phenomenon of heat transfer in nano- and microstructured materials is essential for incorporating such materials in microelectronic and energy conversion devices such as thermopower generators and coolers. Conventionally, the thermal conductivity of bulk materials is determined by measuring the temperature gradient produced by a steady flow of heat in a one-dimensional geometry and is called the steady state method. At lower temperatures (near 300 K), radiation heat loss is small in comparison to the heat transported, and hence the steady state method exhibits acceptable error limits. However, at higher temperatures, black body radiation loss increases and adversely affects the quality of data. Blackbody radiation loss can be reduced by reducing the size of the sample under investigation.¹ The measurement of thermal conductivity by the steady state method becomes increasingly challenging as the sample size decreases to micro- or nanoscale. These difficulties can be reduced by using the technique called the 3ω method, which is less sensitive to errors from blackbody radiation.¹ However, even in the 3ω method, the experimental error on account of black body radiation becomes significant at temperatures above 500 K.

The 3ω method can be used to determine the thermal conductivity of thin films as well as micro/nanowires. The only difference in the determination of the thermal conductivity of the different morphologies is how they are heated.

In the case of a micro/nanowire, the sample (wire) rests on four electrodes without touching the substrate, and the sample itself acts as the heater. In case of thin films, a metal strip along with four electrodes is bonded to the film as a heater. In both arrangements, heating is implemented by passing an alternating current through the sample or the sample heater at an angular frequency of ω , which creates a temperature variation in the sample at a frequency of 2ω that results in a resistance variation also at 2ω . The voltage generated across the sample, being the product of current supplied to the sample and its resistance, therefore varies at 3ω , and hence this method is commonly referred to as a 3ω technique. Such a temperature variation in a wire, heated by an alternating current, was first observed by Corbino,² and later the idea was explored by many scientists, establishing the 3ω technique^{3–11} as an effective tool for the determination of thermal properties of bulk as well as micro- and nanoscale materials.^{12–19}

In the 3ω technique, either a current source or a voltage source can be used to generate a signal across the sample. Lu *et al.*¹⁵ solved the one-dimensional heat equation with the necessary boundary conditions and determined the thermal conductivity of a 20 μm platinum wire and of multiwall carbon nanotube bundles using a current source at room temperature. Choe *et al.*¹⁸ also utilized a current source to measure the thermal conductivity of individual multiwalled carbon nanotubes. Hu *et al.*¹⁶ used the sine output of a lock-in

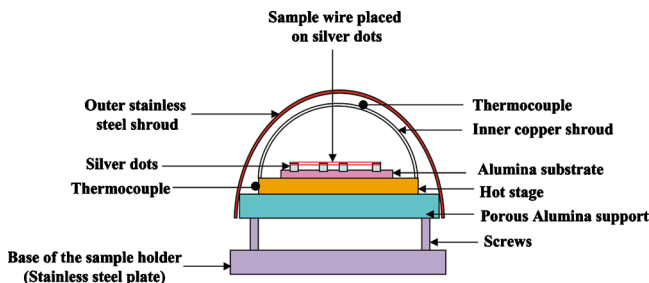
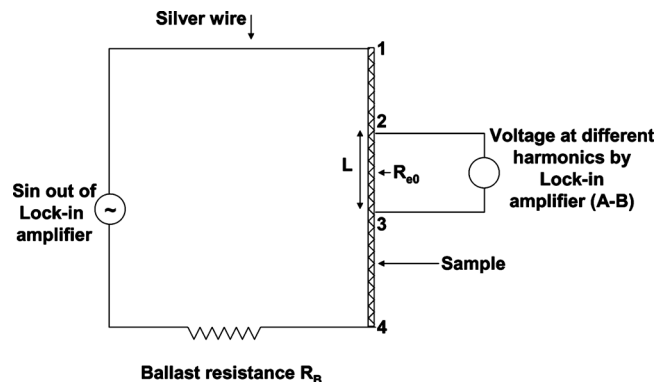


FIG. 1. (Color online) End view of sample mount.

amplifier as a voltage source to measure the thermal conductivity of carbon nanotubes. Holland and Smith⁵ also utilized a voltage source for a microwire. Similarly, Dames and Chen¹² used a voltage source and successfully demonstrated the validity of this technique to determine the thermal conductivity of a platinum microwire and a thin film at room temperature. In the present investigation, by using the sine output of a lock-in amplifier as the voltage source, the thermal conductivity of a 25 μm diameter platinum wire has been determined in the temperature range of 300–725 K using a modified experimental setup.

II. EXPERIMENTAL PROCEDURE

A 25 μm diameter platinum wire, supplied by Omega Engineering, Inc., Stamford, Connecticut, was used as the sample. The wire was mounted as a four-terminal resistor on four silver dots pasted on a polycrystalline alumina (96% Al_2O_3) wafer of 0.5 mm thickness and attached to the dots using colloidal silver paste as shown in Fig. 1. The wire rested on top of the silver dots (electrodes) with a clear air gap between the sample and the alumina substrate. Silver wires attached to the dots serve as the current and voltage leads. A small amount of thermal paste was used to hold the bottom surface of the alumina substrate to a hot stage (ULTRAMIC 600 ceramic heater, Watlow, St. Louis, MO 63146, USA) to perform the experiments at elevated temperatures. The thermal paste ensured good thermal contact between the substrate and the larger, uniformly heated hot stage. The sample temperature was raised to the desired test temperature by applying suitable power to the heater. The Watlow heater, capable of heating to 873 K, consists of a thin film resistor embedded in a ceramic housing and has an integral K-type thermocouple attached to it. In order to minimize radiation loss, the sample and substrate were covered by two reflective heat-shields comprising concentric copper (inner) and stainless steel (outer) shrouds, as shown in Fig. 1. The ends of the semicylindrical copper shroud were in thermal contact with the hot stage, while the stainless steel shroud was separated from but enclosed the copper shroud and was attached to the ends of an insulating porous alumina support upon which the hot stage rests, as shown in Fig. 1. The porous alumina support was mounted to a stainless steel plate with the help of screws and the plate was attached to one of the flanges of the cylindrical vacuum chamber. To minimize the convection loss, a vacuum of $\sim 10^{-5}$ torr was maintained in the sample chamber during the measurement.

FIG. 2. Circuit diagram for thermal conductivity measurement by 3ω method.

The sine output of a lock-in amplifier (SR850, Stanford Research Systems, Sunnyvale, CA 94089) was used as the voltage source ($V_{\text{in-source}}$) so that the phase error between the signal (output) and the input could be minimized. The sinusoidal current, at a frequency of ω , was determined from the source voltage specified by the sine output and was fed to the sample through the outermost electrodes 1 and 4 as shown in Fig. 2. The desired level of current (without heating the sample) at a frequency of ω was determined by adjusting the source voltage at the lock-in amplifier. The 1ω voltage ($V_{1\omega,14}$) generated across the electrodes 1 and 4 in Fig. 2 was measured by the lock-in amplifier along with the voltage generated across the inner two electrodes ($V_{1\omega,23}$). The resistance (R_{14}) of the sample between the outer two electrodes 1 and 4 was calculated by using the source input ($V_{\text{in-source}}$), the 1ω voltage across the outer two electrodes of the sample ($V_{1\omega,14}$) and the resistance, R_B , of the ballast resistor using Eq. (1),

$$R_{14} = \left(\frac{V_{1\omega,14}}{V_{\text{in-source}} - V_{1\omega,14}} \right) R_B. \quad (1)$$

The resistance (R_{e0}) between the inner two electrodes was determined using voltage measurements made while passing a minimal (negligible heating) current through the wire and using Eq. (2) below,

$$R_{e0} = \left(\frac{V_{1\omega,23}}{V_{1\omega,14}} \right) R_{14}. \quad (2)$$

The temperature coefficient of resistance (α) of the sample at a desired temperature (θ_1) was calculated using Eq. (3) after measuring the sample resistances, say, R_{e0,θ_1} and R_{e0,θ_2} , at two slightly different temperatures θ_1 and θ_2 , respectively,

$$\alpha = \frac{R_{e0,\theta_2} - R_{e0,\theta_1}}{R_{e0,\theta_2}(\theta_2 - \theta_1)}. \quad (3)$$

It is necessary to determine a range of input voltages and thus currents, at a frequency of ω , which would yield measurable 3ω signals. The in-phase and out-of-phase 3ω voltages across the inner two electrodes of the sample were measured at a constant frequency for a range of $V_{\text{in-source}}$ and the corresponding 1ω currents. The observed 3ω voltage must be proportional to I^3 as predicted by Eqs. (4) and (5) (see below) for the 3ω method to be applicable. In practice, the

proportionality holds only over a limited range of currents and voltages. This is due to low signal to noise at low voltages and increased radiation losses or other ignored effects at higher voltages. Experimental currents are chosen from the experimentally determined linear region of the curves in order to produce valid data.

For a range of frequencies, the rms values of in-phase ($V_{x,\text{rms}}$) and out-of-phase ($V_{y,\text{rms}}$) 3ω voltages across the inner two electrodes 2 and 3 were measured by the lock-in amplifier for a fixed output voltage (fixed current I) applied at outer electrodes 1 and 4. The measured rms values of the 3ω voltages are related to their respective electrical transfer functions X_3 , and Y_3 , as defined by Dames and Chen,¹² by using the following equations:

$$\text{in-phase electrical transfer function } X_3 = \frac{V_{x,\text{rms}}}{2\alpha R_{e0}^2 I^3}, \quad (4)$$

$$\text{out-of phase electrical transfer function } Y_3 = \frac{V_{y,\text{rms}}}{2\alpha R_{e0}^2 I^3}. \quad (5)$$

The electrical transfer functions are converted into dimensionless in-phase and out-of-phase voltages proportional to the experimentally measured rms 3ω voltages using the defining Eqs. (6) and (7), respectively,

$$\tilde{X}_3 = \frac{12X_3}{R_{\text{th}}}, \quad (6)$$

$$\tilde{Y}_3 = \frac{12Y_3}{R_{\text{th}}}, \quad (7)$$

where thermal resistance R_{th} is defined as

$$R_{\text{th}} = \frac{L}{\lambda A}, \quad (8)$$

where L is the length of the sample between the inner two electrodes, A is the cross-sectional area of the sample wire, and λ is the assumed thermal conductivity of the sample.

Dames and Chen¹² also demonstrated that the thermal transfer function, which depends on the sinusoidal heating of the sample, can be incorporated into the electrical transfer functions. They further noted that a lumped approximation for the thermal transfer function, similar to that for a RC circuit, agrees with the exact solution over the frequency range of interest. Using that lumped approximation, they developed equations for simplified dimensionless theoretical voltages expressed as follows. The theoretical in-phase dimensionless voltage is given by

$$\tilde{X}_3 = \left(-\frac{1}{4} \right) \left(\frac{1}{1 + 4\varpi^2} \right), \quad (9)$$

while the theoretical out-of-phase dimensionless voltage is

$$\tilde{Y}_3 = \left(\frac{1}{4} \right) \left(\frac{2\varpi}{1 + 4\varpi^2} \right), \quad (10)$$

where ϖ is the dimensionless frequency and is given by

$$\varpi = \frac{\omega\tau}{10}, \quad (11)$$

where $\omega = 2\pi f$, f is frequency in hertz, the thermal diffusion time $\tau = L^2/k$, and the thermal diffusivity $k = \lambda/\rho C_p$. Hence, the diffusion time can be expressed as

$$\tau = \frac{L^2 \rho C_p}{\lambda}, \quad (12)$$

where ρ and C_p are the density and the specific heat capacity of the sample, respectively. Theoretical and experimental values of dimensionless 3ω voltages were plotted against the dimensionless frequencies for assumed values of thermal resistance (R_{th}) and thermal diffusion time (τ), both of which are functions of thermal conductivity. The values of density and specific heat capacity were obtained from the literature.¹² Least-squares fits were used to determine the thermal resistance and the diffusion time, which give the best match between theoretical and experimental dimensionless 3ω voltages for both in-phase and out-of-phase components. The values of thermal resistance and diffusion time were obtained from the best fit curves, and the thermal conductivity of the sample is in turn calculated by taking the average of the values obtained using Eq. (12).

III. RESULTS AND DISCUSSION

The major obstacle to performing 3ω measurements at high temperatures (above 500 K) has been the increasing contribution from radiation losses. Minimization of radiation losses from the sample at high temperatures (above 500 K) has been successfully achieved by enclosing the sample by a shroud near the sample temperature and by limiting the radiating surface area of the sample by suitably controlling its

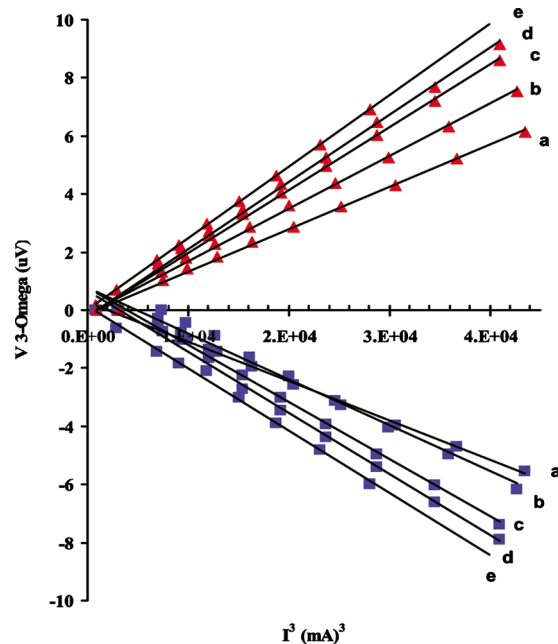


FIG. 3. (Color online) In-phase and out-of-phase 3ω voltage vs cube of the 1ω current, at constant frequency, showing the expected I^3 trend at (a) 300, (b) 400, (c) 500, (d) 600, and (e) 725 K. The squares and triangles represent the in-phase and out-of-phase components of measured 3ω voltages, respectively, and the solid lines are trend lines.

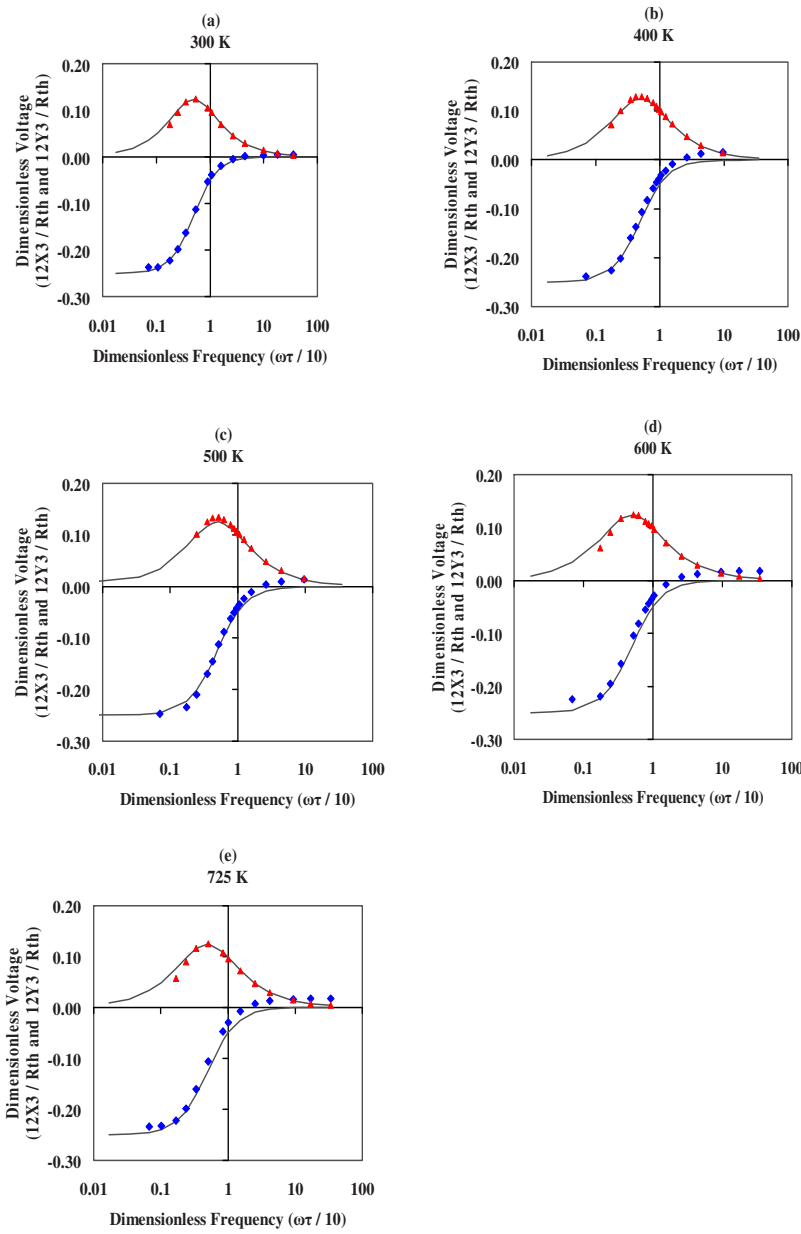


FIG. 4. (Color online) Dimensionless in-phase and out-of-phase $V_{3\omega}$ vs dimensionless frequencies at (a) 300, (b) 400, (c) 500, (d) 600, and (e) 725 K. The solid lines represent the theoretical predictions, and the squares and triangles represent the experimental values of in-phase and out-of-phase components of dimensionless 3ω voltages.

length for a given diameter. The shroud contains two concentric, semicylindrical metal foils (Cu and stainless steel), the stainless steel foil being on the outer periphery. The inside (concave side) of the Cu-foil is lined with a thin shiny Al-foil to increase reflectivity. The edges of the Cu-foil sit on the sample hot stage, which minimized the temperature difference between the stage and the shroud to around 4 K at a measurement temperature of 725 K. The main objective behind using the shroud is to maintain a metallic umbrella over the sample and minimize the temperature difference between the sample and the shroud to eliminate radiation losses to a large extent. To a first approximation, radiation losses are proportional to $T^3\Delta T$, where T is the absolute temperature and ΔT is the temperature difference between the radiating surface and its surroundings. Without thermal shielding, ΔT is ~ 400 K, so reducing it to 4 K represents two orders of magnitude improvement. The radiation losses are further minimized by controlling the length of the sample at a fixed diameter to minimize the radiating surface area.

The measured in-phase and out-of-phase components of the 3ω voltages ($V_{3\omega}$) at a particular frequency are plotted against the cube of the 1ω current (I^3). From Eqs. (4) and (5), a linear relationship is expected between the components of $V_{3\omega}$ and I^3 . We observed the predicted linearity only for a certain range of the sample currents, as shown in Fig. 3. The sample current within the linearity range is applied for further measurements at different frequencies, ranging from 2 Hz to 1 kHz. It is inconvenient to measure the data at lower frequencies because of the long settling times involved. The measured values of 3ω voltages are converted into electrical transfer functions and hence into dimensionless 3ω voltages using Eqs. (6) and (7). The theoretical values of the dimensionless voltages were calculated using Eqs. (9) and (10). The experimental and theoretical values of dimensionless 3ω voltages are compared by using a least-squares fit and are shown in Fig. 4. The assumed values of R_{th} and τ are varied to get the best fit.

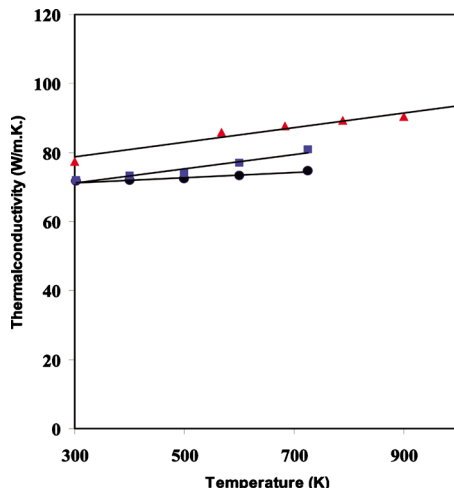


FIG. 5. (Color online) Comparison of values of thermal conductivity of platinum, at different temperatures, obtained from the present investigation on 25 μm wires (squares) and from the literature bulk samples [triangles (Ref. 21) and circles (Ref. 22)] showing the values from present investigation are quite close to the literature. The solid lines are linear fits.

Figure 4 demonstrates the best fit curves for experimental and theoretical values of dimensionless 3ω voltages. The solid lines represent the in-phase and out-of-phase theoretical predictions. The squares represent the in-phase component of experimental dimensionless 3ω voltages, while the triangles represent the out-of-phase components. The values of thermal resistance and diffusion time that gave the best fit curves were utilized in calculating the thermal conductivity of platinum using Eqs. (8) and (12), and the average of these two values of λ is taken to be the thermal conductivity of the sample at that temperature. The five separate plots in Fig. 4 show the fitting of the data taken at different measurement temperatures, i.e., 300, 400, 500, 600, and 725 K. The calculated values of thermal conductivity at a range of temperatures, 300–725 K, are found to vary between 71.8. and 80.8 $\text{W m}^{-1} \text{K}^{-1}$. This investigation shows that thermal conductivity increases monotonically as the measurement temperature increases from 300 to 725 K. Similar results of monotonic increase with temperature of the thermal conductivity of bulk platinum samples by the laser flash method have been reported by Terada *et al.*²¹ By using the 3ω method, Dames and Chen¹² determined the thermal conductivity of 50 μm platinum wire at room temperature to be 70.9 $\text{W m}^{-1} \text{K}^{-1}$; however, measurements of the thermal conductivity of platinum wires by the 3ω technique at higher temperature (~ 725 K) have not been reported previously.

The thermal conductivity of platinum microwire from the present investigation is compared with the data available from different sources in the literature^{20–22} and presented in Fig. 5. The values from the present work fall between the two data sets reported in the CRC Handbook²² and by Terada *et al.*²¹ The values of Terada *et al.* were determined on bulk Pt and are consistently higher than those determined in this investigation, which is consistent with the observation of the

Terada *et al.*, that cold working of platinum (process implemented during drawing of wires) lowers its thermal conductivity. The closeness of the measured value of thermal conductivity in the present work with the literature values demonstrates that the 3ω method can be used as a reliable method for determining thermal conductivity of micro- and nanoscale materials even at high temperatures.

IV. CONCLUSIONS

The thermal conductivity of a 25 μm diameter platinum wire has been determined by the 3ω method over a temperature range of 300–725 K. The problem of radiation losses from the sample at high temperatures (above 500 K), which made the use of 3ω method at high temperature unreliable, has been successfully mitigated by using specially designed shrouds, which equalize the temperature of the sample and the ambience immediately surrounding it. Results of this investigation agree well with published values for bulk platinum and demonstrate that the 3ω method is a promising technique for determining thermal conductivity of metallic microwires not only at room temperature but also at temperatures as high as 725 K.

ACKNOWLEDGMENTS

The authors would like to acknowledge Professor Chris Dames, Department of Mechanical Engineering, University of California, Riverside, California, for his valuable discussions and suggestions.

- ¹D. G. Cahill, *Rev. Sci. Instrum.* **61**, 802 (1990).
- ²O. M. Corbino, *Phys. Z.* **11**, 413 (1910).
- ³L. R. Holland, *J. Appl. Phys.* **34**, 2350 (1963).
- ⁴D. Gerlich, B. Abeles, and R. E. Miller, *J. Appl. Phys.* **36**, 76 (1965).
- ⁵L. R. Holland and R. C. Smith, *J. Appl. Phys.* **37**, 4528 (1966).
- ⁶D. G. Cahill and R. O. Pohl, *Phys. Rev. B* **35**, 4067 (1987).
- ⁷N. O. Birge and S. R. Nagel, *Rev. Sci. Instrum.* **58**, 1464 (1987).
- ⁸D. G. Cahill, E. Fischer, T. Klitsner, E. T. Swartz, and R. O. Pohl, *J. Vac. Sci. Technol. A* **7**, 1259 (1989).
- ⁹D. G. Cahill, M. Katiyar, and J. R. Abelson, *Phys. Rev. B* **50**, 6077 (1994).
- ¹⁰R. Frank, V. Drach, and J. Fricke, *Rev. Sci. Instrum.* **64**, 760 (1993).
- ¹¹D. H. Jung, T. W. Kwon, D. J. Bae, I. K. Moon, and Y. H. Jeong, *Meas. Sci. Technol.* **3**, 475 (1992).
- ¹²C. Dames and G. Chen, *Rev. Sci. Instrum.* **76**, 124902 (2005).
- ¹³T. Kihara, T. Harada, and N. Koshida, *Jpn. J. Appl. Phys., Part 1* **44**, 4084 (2005).
- ¹⁴O. Bourgeois, T. Fournier, and J. Chaussy, *J. Appl. Phys.* **101**, 016104 (2007).
- ¹⁵L. Lu, W. Yi, and D. L. Zhang, *Rev. Sci. Instrum.* **72**, 2996 (2001).
- ¹⁶X. J. Hu, A. A. Padilla, J. Xu, T. S. Fisher, and K. E. Goodson, *J. Heat Transfer* **128**, 1109 (2006).
- ¹⁷T. Y. Choi, M. H. Maneshian, B. Kang, W. S. Chang, C. S. Han, and D. Poulikakos, *Nanotechnology* **20**, 315706 (2009).
- ¹⁸T. Y. Choi and D. Poulikakos, *Appl. Phys. Lett.* **87**, 013108 (2005).
- ¹⁹T. Y. Choi, D. Poulikakos, J. Tharian, and U. Sennhauser, *Nano Lett.* **6**, 1589 (2006).
- ²⁰Thermophysical Properties Research Center, Perdue University, *Thermophysical Properties of Matter*, edited by Y. S. Touloukian (IFI/Plenum, New York, 1970).
- ²¹Yoshihiro Terada, Kenji Ohkubo, and Tetsuo Mohri, *Platinum Met. Rev.* **49**, 21 (2005).
- ²²David R. Lide, *CRC Handbook of Chemistry and Physics*, 76th ed. (CRC, Boca Raton, FL, 1996), pp. 12–175.